

Fast WDM provisioning with minimal probing: the first field experiments for DC exchanges

HIDEKI NISHIZAWA,^{1,*} TORU MANO,¹ THOMAS FERREIRA DE LIMA,² YUE-KAI HUANG,² ZEHAO WANG,³ WATARU ISHIDA,⁴ MASAHISA KAWASHIMA,⁵ EZRA IP,² ANDREA D'AMICO,⁵ SEIJI OKAMOTO,¹ TAKERU INOUE,¹ KAZUYA ANAZAWA,¹ VITTORIO CURRI,⁵ GIL ZUSSMAN,⁶ DANIEL KILPER,⁷ TINGJUN CHEN,³ TING WANG,² KOJI ASAHI,⁹ KOICHI TAKASUGI¹

¹NTT Network Innovation Labs, Kanagawa, Japan, ²NEC Labs America, Princeton, USA, ³Duke University, Durham, NC, USA, ⁴NTT Software Innovation Center, Tokyo, Japan, ⁵NTT IOWN Development Center, Tokyo, Japan, ⁶Politecnico di Torino, Torino, Italy, ⁷Columbia University, New York, USA, ⁸CONNECT Centre, Trinity College Dublin, Ireland, ⁹NEC Corporation, Chiba, Japan.

*Corresponding author: hideki.nishizawa@ntt.com

There are growing expectations for data center interconnection (DCI) services, which use optical fiber to connect any DC distributed in a metro area and quickly establish high-capacity optical paths between each company's cloud services and carrier mobile edge computing (MEC) and the users connected to them. In such networks, a coherent transceivers with various optical frequency ranges, modulators, and modulation formats installed at each connection point must be used to meet service requirements such as fast-varying traffic requests between user computing resources and rapid recovery during a disaster. This requires technology and architectures that allow users and DCI network operators to cooperate to achieve fast provisioning of WDM links and flexible route switching in a short time, independent of the transceiver's implementation and characteristics. We propose an approach to estimate the end-to-end GSNR accurately in a short time when a DCI network operator receives a service request from users, not by measuring the GSNR at the operational route and wavelength for the End-End optical path but by simply applying a QoT probe channel link by link, at a convenient wavelength/modulation-format for measurement. Assuming connections between coherent transceivers of various frequency ranges, modulators, and modulation formats, we propose a new device software architecture in which the DCI network operator optimizes the transmission mode between user transceivers with high accuracy using only standard parameters such as Bit Error Rate (BER). In this paper, we first experimentally built three different routes of 32 km/72 km/122 km in the C-band to confirm the accuracy of this approach. For the operational end-to-end GSNR measurements, the accuracy estimated from the sum of the measurements for each link was 0.6 dB, and the wavelength-dependent error was about 0.2 dB. Then, using field fibers deployed in the NSF COSMOS testbed (deployed in an urban area), a Linux-based transmission device software architecture, and coherent transceivers with different optical frequency ranges, modulators, and modulation formats, the fast WDM provisioning of an optical path was completed within 6 minutes (with a Q-factor error of about 0.7 dB).

1. INTRODUCTIONS

A. Emerging Expectations for DCX

While cloud services are expanding, efforts to relocate data centers previously concentrated in urban areas to suburban areas with abundant power and infrastructure space are increasing to equalize regional energy supplies. Sovereign clouds, which keep data within a designated geographic area to improve data security and privacy, are also becoming more prevalent. In addition, the growing use of private 5G technology has increased the need for high-speed, low-latency optical links between remote locations. In fact, there are increasing cases where data owned in local data centers are connected to cloud services and Mobile Edge Computing (MEC) using dark fiber and

high-capacity optical links. However, these demands are met with significant challenges, such as the time it takes to procure dark fiber and start using the network, and the complexity and cost of the network increases as the number of locations to be connected increases.

Against this backdrop, there are growing expectations for DC Exchange (DCX) services that directly connect any DCs distributed in a metro area via optical fiber to quickly establish high-capacity optical paths between each company's cloud services and MECs and the users connected to them [1].

Fig. 1 shows an example of a DCX configuration. Urban Data Centers (UDCs) are located in the gray area in the center of Fig. 1, and they are connected by Carrier Links (CLs) owned by the carrier, which provides a Point of Presence (POP) in each UDC. User equipment can connect from a Suburban Data Center (SDC)

to the POP in UDC via Alien Access Links (AALs) and directly to a remote cloud MEC or other user equipment without electrical conversion. Here, the user equipment can be located at either SDC or UDC, and if it is at UDC, it connects directly to the POP without an access line.

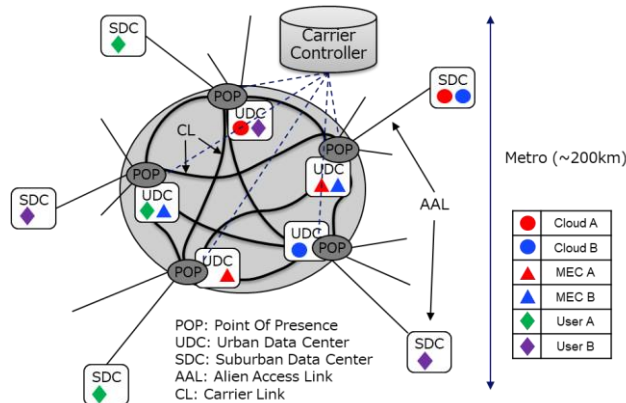


Fig. 1. DCX physical deployment example.

B. Service Requirements for DCX

There are challenges to realizing the DCX services that require real-time WDM provisioning to quickly fulfill user demand, and protocols to enable user-carrier cooperation automatically. Also, when a failure occurs in a user TRx installed outside the carrier network, the carrier needs to isolate the root cause and perform restoration work. The service requirements for DCX are broken down as follows:

- (1) Rapid response to fast time-varying traffic requests that occur between DCs;
- (2) Prompt optical path restoration in the event of disasters such as earthquakes and floods;
- (3) Support for ultra-low latency services for inter-computer communications;
- (4) Direct connection between various devices installed at user sites, cloud, and MECs without optical-electrical conversion; and
- (5) Monitoring and control of user equipment by carriers to ensure stable operation of network services.

Here, the target response time required for (1) and (2) set to be around 10 minutes (For (2), the case where the QoT of multiple optical links are degraded at once is included, and this target is defined as the time required to restore one end-to-end (EtE) optical path between a particular user's muxponder). The latency in (3) is assumed to be within 2 ms, dominated by fiber propagation delay. This delay corresponds to a metro area of roughly 200 km in radius, depending on the fiber installation conditions.

C. Importance of Open Interface/Specification

To address the requirements (1) ~ (4) described in Section B, we must design an open architecture that enables fast WDM provisioning between various devices. The architecture should allow DCX operators to exchange telemetry information to calculate the Quality of Transmission (QoT) of each link in real-time, independent of the vendor or implementation of each device. This requires an accurate estimation of the generalized signal-to-noise ratio (GSNR) that shows the signal quality at the physical layer in all possible transmission channels between the user sites.

To address the requirements (4) (5) described in section B among users, clouds, and MECs, interoperability is a critical issue because, generally, each player uses their preferred devices that adapt to their system and operation.

Some standardization organizations such as Optical Internetworking Forum (OIF) [2], Open ROADMSA [3], and OpenZR+ MSA [4] recently defined common hardware specifications for data plane interoperability. As for control plane interoperability, there is no common specification that addresses the service requirements for DCX among the optical transport industry, while OpenROADMSA, Telecom Infra Project Open Optical & Packet Transport (TIP OOPT) [5, 6, 7], and IOWN Global Forum (IGF) [8] give architectures and open interfaces that partially meet these needs identified here.

D. Fast WDM Provisioning Approach based on Open Architecture

In this paper, we propose a fast WDM provisioning approach for WDM links, including two types of commercial TRxs implemented with Indium Phosphide (InP) and Silicon Photonics (SiP) modulators. Our approach uses a technique to estimate the GSNR of all possible EtE optical paths quickly and accurately by only using a probe WDM channel that measures QoT link by link at measurable, convenient arbitrary modulation formats and modulators.

We have verified a minimal probing method and an integrated Linux-based device software architecture that utilizes open interfaces, specifications, and architectures defined by Open ROADMSA, TIP OOPT, and IGF. We leverage Open ROADMSA-compliant coherent TRxs to ensure data plane interconnectivity. For the hardware abstraction interface and network operating system (NOS) that controls user TRxs, we applied the TAI architecture and the Goldstone NOS that are under development openly in TIP OOPT. The architecture proposed in the IGF was adopted for the network architecture of user TRx and POP. We implement software libraries for fast WDM provisioning, and monitoring/configuration of the user's TRx to realize control plane interoperability. The proposed device software architecture solves the issue currently not supported by standard YANG models, such as the Open ROADMSA YANG model and the OpenConfig YANG model. By utilizing server-based technologies such as containers and the hardware abstraction interface for coherent modules and optimizing only common parameters (BER, modulation format, and baud rate), enhanced remote control of user TRxs can be achieved without modifying the existing TRx MSA.

In addition, we experimentally confirmed the accuracy of this approach using three different routes of 32 km/72 km/122 km in the C-band. For the operational EtE GSNR measurements, the accuracy estimated from the sum of the measurements for each link was 0.6 dB, and the wavelength-dependent error was about 0.2 dB. Then, using field fibers deployed in an urban area, a Linux-based transmission device software architecture, and coherent transceivers with different optical frequency ranges, modulators, and modulation formats, the fast WDM provisioning of an optical path was completed within 6 minutes.

The paper is organized as follows. After introducing related works in Section 2, we propose our approach to estimating the GSNR of all possible EtE optical paths quickly with high accuracy in Section 3. Section 4 presents a Linux-based muxponder device software architecture that includes a DCX operator agent as a container. The architecture also allows optimization of different settings of coherent transceivers (TRxs) from multiple vendors with different optical frequency ranges and modulators. In

Section 5, we evaluate and compare the estimation error of this method and the penalty due to wavelength dependence and wavelength assignment of the device against the actual end-to-end GSNR measurements. In Section 6, we report the time measurements for quality estimation of each link, EtE optical path margin design, and remote configuration of user muxponders using an experimental setup containing field fibers. Section 7 discusses future challenges for improving accuracy and expanding system flexibility, and a conclusion is provided in Section 8.

2. RELATED WORK

Research on quickly establishing high-capacity optical paths between distributed DCs in a metro area is discussed in the literature [9]. It introduces a converged inter/intra data center network architecture with an autonomous control plane for flexible bandwidth allocation. It has two types of physical layer connections (Background and Dynamic) to meet stringent bandwidth and delay requirements. Next, [10] targets the provisioning of disaster-resilient cloud services using distance adaptive modulation formats by simultaneously considering content placement, modulation-format adaptive routing, path and content protection, and spectrum allocation. It investigates frequency utilization with different traffic parameters and different network topologies by numerical simulations. However, neither prior work considers the WDM provisioning approach.

Several papers have been published by K. Kaeval et al. on transmission mode optimization approaches for WDM provisioning [11, 12, 13]. They propose an approach for provisioning WDM using QoT probe channels in a transparent optical path connecting two endpoints in a single or multi-domain optical network called optical spectrum as a service (OsaaS). K. Kaeval et al. estimate the GSNR in EtoE between TRxs of OsaaS users in [11, 12], and an approach is proposed to estimate the GSNR EtoE using the estimated GSNR for each link that constitutes the EtoE route [13]. In both cases, the GSNR is estimated for each wavelength using a probe channel with the same wavelength as the signal light in operation, which requires time for provisioning in the case of multi-wavelength multiplexed transmission. Furthermore, while OsaaS is a P-to-P connection, DCX is a many-to-many connection deployed on a two-dimensional plane, as shown in Fig. 2(b), so the model is more complex than [13] with many combinations of optical path routes and wavelengths. The differences between the models are discussed in detail in Section 3. The OsaaS work does not consider an architecture for users and carriers to work together when setting WDM paths. Furthermore, a single vendor device is applied to the transmitter and receiver, and no study or experiment was conducted to set up optical paths between optical transmission devices with various optical frequency ranges, modulators, and modulation formats installed at each connection point, such as DCX. This is discussed in detail in Section 4.

An architecture for users and carriers to work together using optical transmission devices with optical frequency range and modulation format has been proposed in [14]. Here, an architecture and protocol are proposed in which a mode catalog, including the modulation format and characteristics of the coherent TRx, is generated at the user site, the QoT of the link is estimated, and these are sent to the carrier's controller for optimization and configuration of the user site equipment. [15] described that the back-to-back characteristics of coherent TRxs

can be accurately modeled for different types of coherent implementations and modulators. However, [14] and [15] do not mention network topology, specific steps for mode optimization, or a device software architecture for user TRx remote control, and only laboratory experiments have been conducted.

3. GSNR estimation of all possible EtE optical paths in a short time with high accuracy

This Section presents an approach to achieve WDM provisioning and select the optimal mode in a short time, which is essential to achieve service requirements (1) – (4).

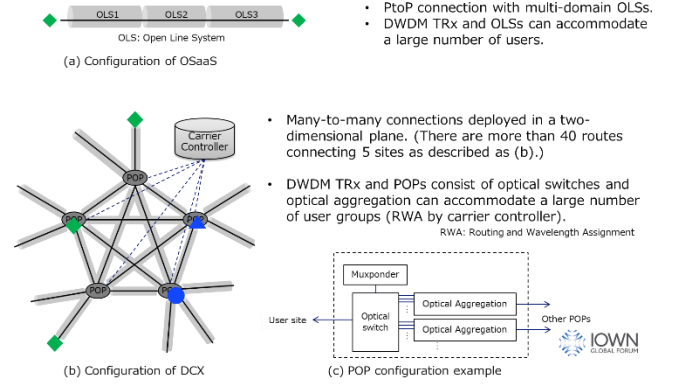


Fig. 2. Example network configuration of DCX.

Fig. 2 (a) shows the OSaaS configuration [11]. It consists of a multi-domain Open Line System (OLS) and can accommodate many users by applying DWDM. Fig. 2(b) shows an example of a network forming a DCX, in which a functionally disaggregated ROADM device [8] consisting of an optical switch and optical aggregation is applied to the POP in Fig. 2 (c). Same as Fig. 2 (a), DCX can efficiently accommodate many user groups with DWDM technologies.

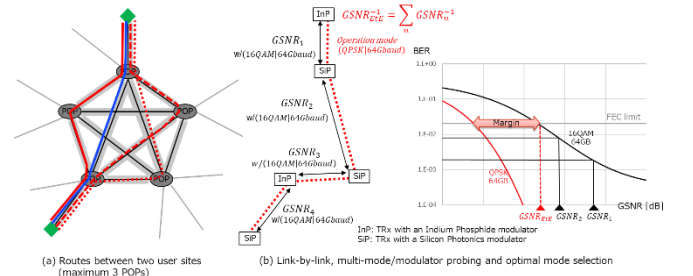


Fig. 3. Approach to select the optimal mode with high accuracy in a short time.

Fig. 3 (a) shows possible patterns in which two user sites could be connected via DCX. If we limit the number of POPs between user sites to three to minimize latency, there are four patterns as in Fig. 3 (a) (two POPs: blue line, three POPs: three red lines). When connecting the 5 POP sites shown in Figure 2 (b), there are more than 40 possible patterns. In order to satisfy the service requirements (1) ~ (4) shown in Section 1, the EtE GSNR between each site must be determined accurately. The optimal mode must be selected in a short time (here, we assume that existing techniques can be applied to Routing and Wavelength Assignment (RWA) and focus our discussion in this paper on the fiber propagation design of the WDM optical path.).

We have previously confirmed in [15] that the back-to-back characteristics of coherent TRxs can be accurately modeled according to equations (1) and (2) for various modulation formats, baud rates, and modulator types. Doing so allows the Gaussian noise approximation to be applied in the metro region as well as the long haul. Equation (1) relates the BER to the back-to-back GSNR as a function of each modulation format, such as 16QAM or QPSK, and Eq. (2) shows two examples of error functions. Equation (3) shows that the reciprocal of the GSNR is simply the sum of the reciprocal contributions of three SNR terms originating from three noise sources: intrinsic TRx characteristics, spontaneous emission of the amplifier, and fiber nonlinear optical effects.

$$BER = \Psi_{MF}(GSNR) \quad (1)$$

$$\Psi_{MF} = \frac{3}{8} \operatorname{erfc}\left(\frac{\sqrt{GSNR}}{10}\right) \text{ for } 16QAM, \frac{1}{2} \operatorname{erfc}\left(\frac{\sqrt{GSNR}}{2}\right) \text{ for } QPSK \quad (2)$$

$$GSNR^{-1} = SNR_{TRx}^{-1} + SNR_{ASE}^{-1} + SNR_{NLI}^{-1} \quad (3)$$

In [15], we have also experimented with two types of commercial TRxs implemented with InP and SiP modulators and have verified that means. (1) ~ (3) were valid for both modulators. Furthermore, we assume that the reciprocal of the EtE GSNR is equal to the sum of the reciprocal of the GSNRs of each link, as in Eq. (4). Although it has been reported by [13] that this equation is valid with an accuracy of ± 1.4 dB for the 3116 km transmission in the case of Fig. 2 (a), no experiments have yet been performed to verify the accuracy in the case of Fig. 2 (b).

$$\begin{aligned} GSNR_{EtE}^{-1} &= SNR_{TRx}^{-1} + \sum_n \{SNR_{ASE,n}^{-1} + SNR_{NLI,n}^{-1}\} \\ &= SNR_{TRx}^{-1} + \sum_n GSNR_{LS,n}^{-1} \end{aligned} \quad (4)$$

Using these results, the EtE GSNR of a potential path can be estimated in a short time without direct measurement of the QoT, regardless of the modulation format and modulator type of TRx. Fig. 3(b) shows the steps to measure QoT on a link-by-link basis for one of the routes in Fig. 3 (a) using a measurably convenient mode and multiple types of modulators and then calculate the EtE GSNR to select the operational mode. For example, $GSNR_1$ is measured between TRx with InP and SiP modulators. Since the QoT is relatively high for a single span, BER is measured with 16QAM 64Gbaud mode and converted to GSNR (the method for obtaining SNR_{TRx} is discussed in Section 4). $GSNR_{EtE}$ is then calculated by summing the link-by-link reciprocal GSNRs, and the optimal mode can be selected after adding the operational margin [16]. In this example, $GSNR_n$ is estimated using 16QAM 64Gbaud, and QPSK 64Gbaud is selected by adding an operational margin to the calculated $GSNR_{EtE}$. Since this approach uses common parameters (BER, modulation format, and Baud rate), that can be applied to all coherent TRx without being restricted to a specific device.

4. Device software architecture

The discussion in Section 3 has enabled the selection of a feasible and optimal transmission mode from a fiber propagation design viewpoint. However, there are still issues to be addressed in satisfying (4) and (5) in Section 1 B; the remaining issues are discussed in this Section.

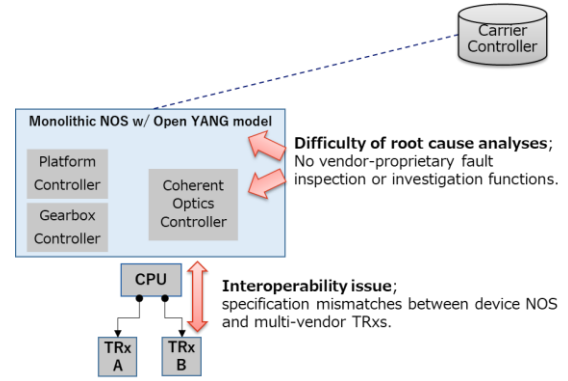


Fig. 4. Issues in user TRx remote control.

Figure 4 shows the issues when the carrier remotely controls the user TRx as a DCX servicer.

Difficulty of root cause analyses: If a failure occurs at a user site after the service has been launched, the carrier, as a DCX service provider, is required to isolate the failure on its own. The approach for the carrier to monitor and control the TRx at the user site would be to manage the TRx from the controller via NOS using an open YANG model or implementing a remote monitoring and control function within the TRx. However, no open specification is defined to monitor and control the TRx installed in user sites utilizing vendor-proprietary fault inspection or investigation functions. Though there are some activities to enhance traditional standardized YANG models for network design and operation automation [17], there is no definition for utilizing vendor-proprietary functions on them.

Interoperability issue: To ensure the safe operation of network services, accidents caused by device connectivity must be avoided. For example, when using TRxs from multiple vendors, accidents can occur due to specification mismatches between the NOS and the TRx, resulting in optical power input from the user device exceeding the regulated value or signals with unexpected optical frequency being input into the network during network connection. In fact, even for TRxs with a specified MSA, there are cases where vendors implement specifications outside the MSA to meet their customers' requirements, and then there may be cases where the units of parameters differ between vendors in terms of dBm or linear power (mW). Also, since each vendor TRx has a different optical frequency range, the optical frequency corresponding to f_1 defined by the vendor is different for each vendor. For the reasons stated above, it is difficult for carriers to remotely restore the system when a failure occurs due to a specification mismatch between the NOS and TRx at a user site.

In this paper, we propose a device software architecture to solve the problem which currently is not supported by the standard YANG model (Note that the physical network connection method for control signal between the controller and the user muxponder and the user authentication method is outside the scope of this paper.).

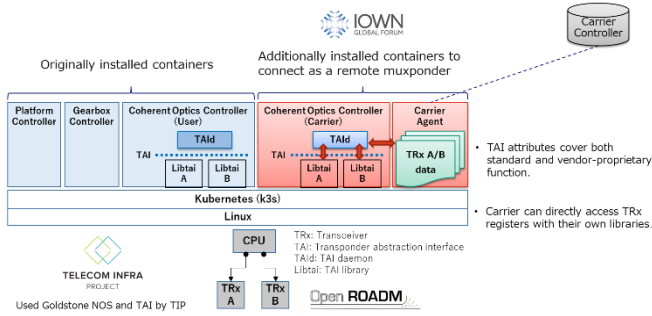


Fig. 5. Example of container-based device software architecture.

Figure 5 shows the device software architecture used in this experiment, which allows the carrier to monitor and control a TRx in the user muxponder. The hardware was Phoenix [5], as specified in the TIP OOPT, and the TRx was based on the OpenROADM MSA specification [3]. Two CFP2-DCOs from vendors (A and B in the Fig. 5) were applied. The IGF's disaggregated architecture described in the Open All-Photonics Network (APN) Functional Architecture [8] was used for the user muxponder and ROADM network configuration. The device software used was the NEC NOS, developed based on the Goldstone NOS [6] at the TIP OOPT Github site. Gearbox and Coherent Optics control functions are implemented as containers. In this experiment, the Carrier's Coherent Optics Controller and Carrier agent (red) were added as containers in addition to the group of containers initially installed on the User muxponder (blue).

The TAI architecture hides the differences among various TRx form factors or vendors. It consists of a library called libTAI that absorbs these differences and an open interface, which allows TAI to monitor and control TRx A/B agnostically in regard to form factor type or vendor type. We developed LibTAI for TRx A/B and used it in this experiment, and then performed mode optimization between various devices using the standard parameters (BER, modulation format, and Baud rate). Since only standard parameters are used for mode optimization, we can do it on any standard TRxs.

TAI is designed to add attributes for using vendor-proprietary functions as well as attributes for standard functions. The carrier can remotely control these containers and directly access the user's TRx registers with TAI and an in-house library to guarantee the safe operation and robustness of the DCX. For

example, the CFP MSA defines a module vendor private register [18]. Vendors use this to provide their proprietary functions, conducting pre-shipment inspections and root cause investigations for unexpected faults. Suppose carrier controllers can take advantage of this capability with containers. In that case, carriers can use this information to conduct more advanced root cause investigations in case of a fault without requesting the actions of the user. Furthermore, carriers and users do not need to disclose source code to each other by utilizing containers with executable binaries, and operational management, such as firmware updates, can be performed immediately and independently. Note that the automatic firmware upgrade of the coherent module has been demonstrated in a multi-vendor environment [19].

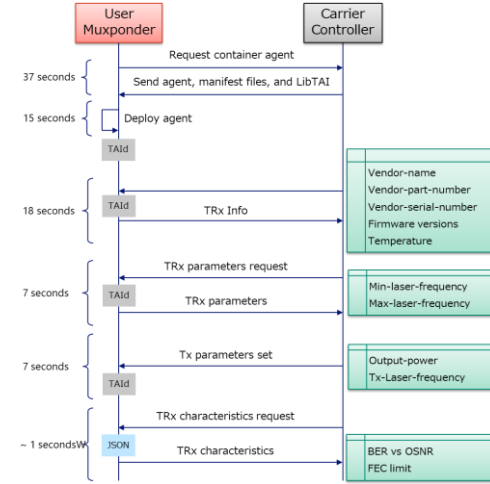


Fig. 6. Monitoring and control of TRx in User muxponder by carrier.

Fig. 6 shows an example of User muxponder control by the carrier. When the User muxponder connects to the DCX, it obtains and installs the necessary container from the carrier controller and sends TRx data such as vendor name, firmware version, and parameters to the carrier controller. The carrier controller then checks to see whether the TRx is certified and requests TRx characteristic information from the User muxponder in case it has been executed. We assume that an

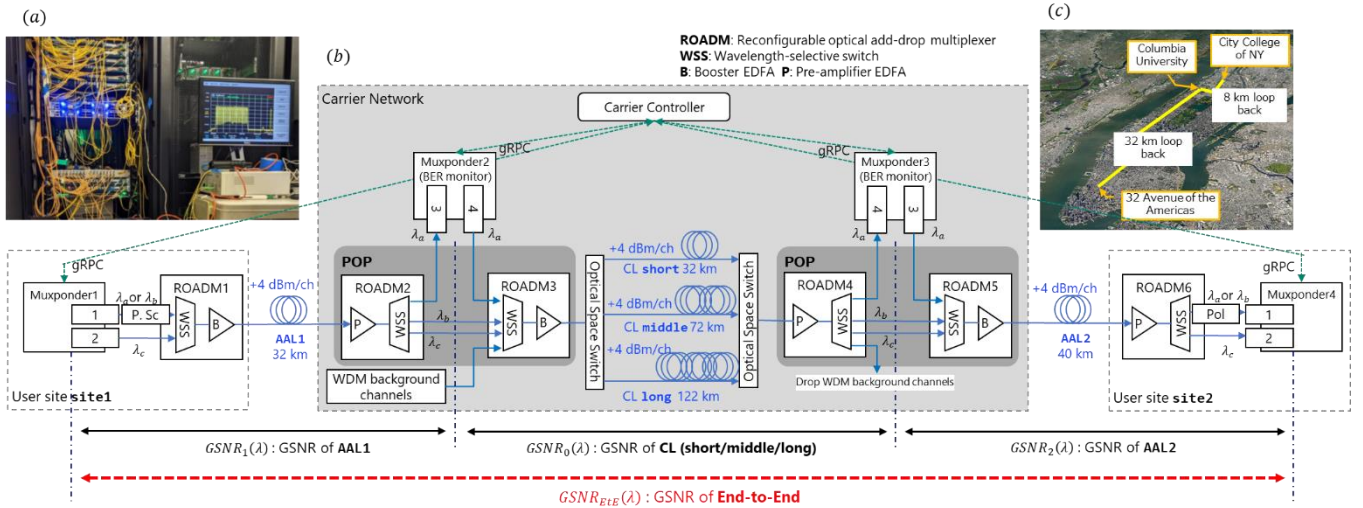


Fig. 7: (a) Equipment in COSMOS testbed. (b) Field trial setup. (c) Field fibers.

executed non-disclosure agreement is in place between the carrier and the TRx vendor [20]. There are several possible approaches for vendors to provide TRx characteristics data. For example, some TRx vendors store back-to-back BER vs. OSNR and other characteristics in registers in the TRx at shipment. In this experiment, we stored these characteristics as a JSON file in the user muxponder. The time required to implement and complete the sequence shown in Fig. 6 was measured to be 90 seconds, and it was confirmed that the time required was short enough.

5. EtE GSNR measurement results and estimation errors

This Section presents the results of evaluating the errors of the link-by-link measurement approach introduced in Section 3, as well as wavelength dependence and Q-value variation, using commercial open systems and field fibers.

A. Experimental Setup

Fig. 7 (a) and (b) show the field trial setup using the NSF COSMOS testbed, a city-scale programmable testbed deployed in Harlem, NYC. The COSMOS testbed provides a programmable optical networking environment, including optical space switches and Lumentum ROADM-20 units, where many experimental results have been created [21, 22, 23]. We experimentally construct two user sites, two POPs, AAL1, AAL2, and CL, with three different paths of 32 km/72 km/122 km in the C-band by utilizing commercial optical transmission devices and field fibers. We deployed white box muxponders, which comply with TIP's Phoenix requirements [5], and installed NEC's network operating system (NOS), which is based on the TIP Goldstone NOS [6]. These muxponders utilize Open ROADM compliant 400G CFP2-DCO pluggable transceivers from Fujitsu Optical Components and Lumentum. Fig. 7 (c) shows the Manhattan dark fiber routes we used in this experiment; 32 km loop-back field fibers between Columbia University and a colocation data center at 32 Avenue of the Americas (provided by Boldyn), and an 8km loop-back field fiber between Columbia University and the City College of New York (provided by CrownCastle). The first AAL, AAL1, consists of a ROADM and a 32 km field fiber and connects to a CL. The second AAL, AAL2, consists of a ROADM and 40 km spool fiber. The CLs have different lengths and losses for different link conditions, with a total of 25 WDM background channels inserted to emulate existing in-service channels (Details are described later in Section C). All input powers to the fiber links were +4

dBm/channel. Two muxponders are placed at the POPs, interfacing AAL and CL for pre-FEC BER probing measurements. The controller interacts with the muxponders in user sites and POPs through a pre-established secure channel using gRPC.

B. Link-by-link measurement error

To check the error of the approach shown in Fig. 3(b), we compared the measured EtE GSNR ($GSNR_{EtE}$) and estimated GSNR with link-by-link measurement ($GSNR_1/GSNR_0/GSNR_2$) in Fig. 7 (b). We plotted the results in Fig. 8, where GSNR_all on the vertical axis corresponds to the entire GSNR, including the GSNR of the TRx and Link.

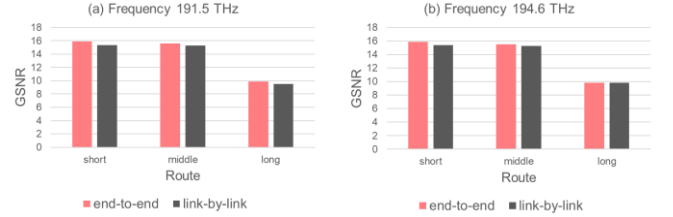


Fig. 8. Measured EtE GSNR and estimated GSNR with link-by-link measurement.

The bar graph on the left and the right of Fig. 8 show the difference between the two GSNRs with 191.5 THz and 194.6 THz, respectively. We changed the CL with the optical space switch and evaluated it in three route patterns: short, middle, and long. There were no significant differences in wavelength or CL distance, with errors ranging from 0.3 to 0.6 dB.

C. Wavelength-dependent error

Fig. 9 shows the experimental system configuration with an inset showing the WDM spectrum assignment. To measure the wavelength dependence of the link system, we established probing channels listed in the table in Fig. 9 between muxponder 2 and muxponder 3. We changed the CL with the optical space switch. We evaluated it in three patterns: short, middle, and long, with 25 WDM background channels with 100 GHz spacing (see the background channels table in Fig. 9.) inserted to emulate existing in-service channels. To verify if λ_a (191.5 THz, at the edge of the C-band) can be utilized as a probe signal for channels of other wavelengths, we compared the difference between the GSNR measured at λ_a and the GSNR measured at different wavelengths (b, c, d, e). The wavelength-dependent error on GSNR probing caused by the line system was 0.05 dB, 0.11 dB, and 0.22 dB at the short, center, and long routes, respectively.

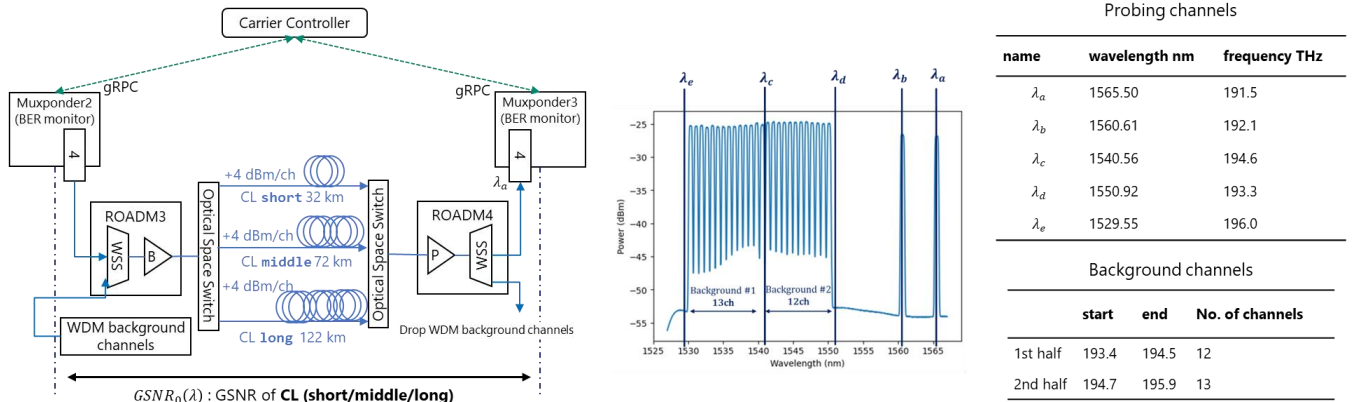


Fig. 9. Experimental set-up for wavelength-dependent error measurement.

Although λ_c is located in the center of the background channels, no significant difference from λ_a and other wavelengths was observed. This suggests that the waveform degradation due to fiber nonlinear effects was relatively small for the system compared to the noise contribution of the TRx back-to-back characteristics, as expected for this metro-scale system.

D. GSNR fluctuation of the system

The measured value of GSNR in the experimental system is constantly fluctuating. Since the estimation error cannot be smaller than this fluctuation, we evaluated the amount of fluctuation. We measured the GSNR every 5 seconds at three links (AAL1, AAL2, CL1) and EtE path (EtE) and calculated the amount of fluctuation of the 5-minute moving average. We define the amount of GSNR fluctuation as the difference between the 5th and 95th percentile of the 5-minute moving average. The measurement duration was seven days.

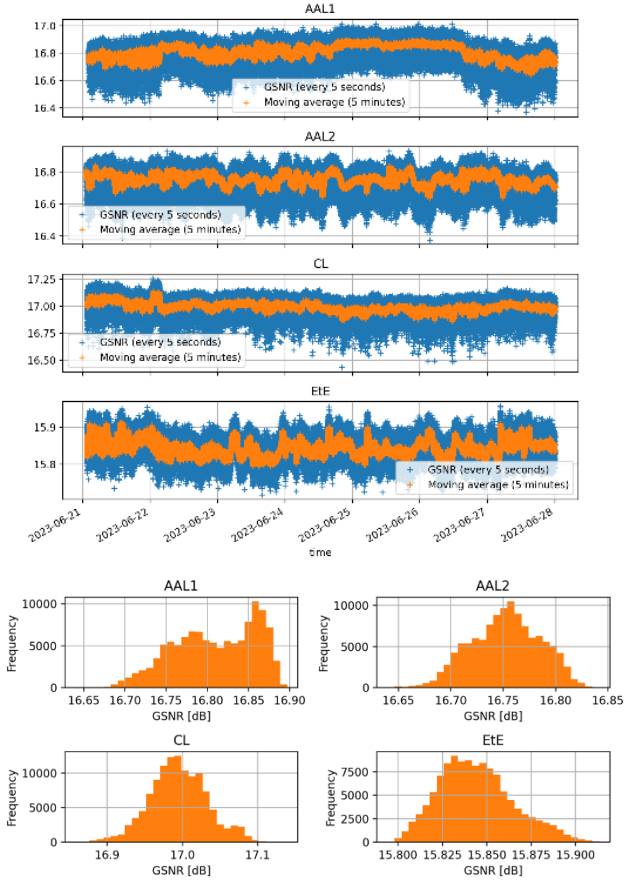


Fig. 10. Time variations of GSNR (top) and histograms of 5-minute moving average (bottom)

The GSNR every 5 seconds varied by about 0.2 dB to 0.4 dB over time (Fig. 10). Since we usually use the average value over several observations, we evaluated the fluctuating amount of the moving average. We set the average window period as 5 minutes. The 5-minute moving average fluctuated from about 0.1 dB to 0.2 dB over time (Fig. 10). The amount of GSNR fluctuations for AAL1, AAL2, CL, and EtE are 0.15, 0.10, 0.07, and 0.07 dB, respectively (Fig. 10). The amount of GSNR fluctuation is roughly 0.1 dB to 0.2 dB.

E. Summary of error estimated results

Table 1 shows the error estimated results with our experimental setup in Fig. 7. The overall margin required for fast WDM provisioning using the link-by-link approach and probe light of any wavelength was 0.7 dB. This value is the same order of magnitude of the system's GSNR fluctuation, roughly 0.1 dB to 0.2 dB, so any available wavelength can be used in conducting the approach shown in Fig. 3 with a small margin.

Transmission distance	LbL measurement error	WL-dependent error	Required margin
~100 km	0.60 dB	0.05 dB	0.65 dB
~150 km	0.32 dB	0.11 dB	0.43 dB
~200 km	0.47 dB	0.22 dB	0.69 dB

Tab. 1. Error estimated results.

6. Results of fast WDM provisioning experiments using field fibers

In this Section, we apply the proposed architecture and evaluate the time required for quality estimation of each link, EtE optical path margin designing, and remote configuration of the user muxponder, with two routes (short and long) using field fiber on Fig. 7 (C).

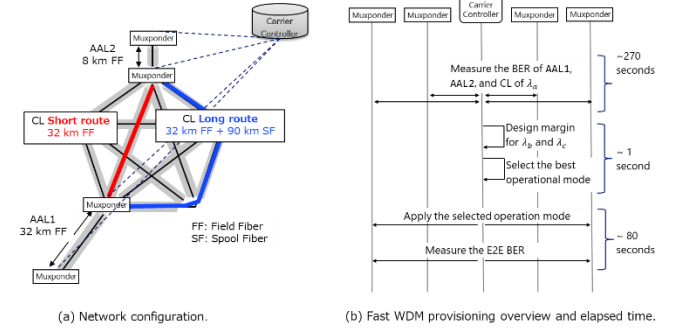


Fig. 11. Fast WDM provisioning experiment.

Fig. 11(a) shows this experiment's network configuration. The route shown in Fig. 11(a) was applied to AAL1, CL, and AAL2 in the experimental configuration shown in Fig. 7. Two dark fiber routes (32 km and 8 km) in Fig. 7 (c) were used. The short CL (32 km field fiber) and long CL (32 km field fiber + 90 km spool fiber) have different lengths and losses for different link conditions, with a total of 25 WDM background channels inserted to emulate existing in-service channels (same as Fig. 9). Fig. 11 (b) shows an overview of fast WDM provisioning and elapsed time. The controller gathered JSON-formatted TRx characteristics from all muxponders then measured the BER of AAL1, AAL2, and CL with the muxponders. We used λ_a (191.5 THz) as a probing signal. The controller calculates the margins using the approach in Fig. 3(b) and selects the best operational mode. Finally, the controller configures the operation mode to the user muxponders and measures the EtE BER. The total provisioning time was 351 seconds, broken down as follows. Link BER measurements took 270 seconds, margin design and mode selection took under one second, and user muxponder configuration and BER measurement took 80 seconds.

Tab. 2: Measured BER (GSNR)

Route	GSNR_Is		
	AAL1	CL	AAL2
Short	1.24e-3 (23.3 dB)	1.03e-3 (23.9 dB)	5.64e-4 (27.2 dB)
Long	1.14e-3 (23.6 dB)	1.75e-3 (12.4 dB)	1.21e-3 (23.0dB)

Table 3: Estimated GSNR EtE, selected mode, secured margin, estimated Q-factor, and measured Q-factor

Route	Ch	GSNR_Is	Mode	Margin	Est. Q	Mes. Q
Short	λ_b	19.7 dB	400G	5.2 dB	dB	9.40 dB
Long	λ_b	11.7 dB	200G	5.1 dB	dB	11.2 dB
Long	λ_c	11.6 dB	200G	4.9 dB	dB	10.9 dB

We provisioned two routes, short and long, assuming a 400G bandwidth request from a user. Tab. 2 shows the measured BER and converted GSNR for AAL1, CL, and AAL2. Combining these measured GSNR values, our controller estimated EtE GSNR and provisioned the optical paths (Tab. 3). As for the short route, our controller successfully selected the single 400G DP-16QAM path using λ_b with a 5.2 dB secured GSNR margin. As for the detour route, our controller also successfully selected the two 200G DP-QPSK paths using λ_b and λ_c since 400G DP-16QAM is not error-free due to the low EtE GSNR. The secured margins for these two paths were 5.1 dB and 4.9 dB. In all cases, the differences between the estimated and measured Q-factor (BER) were less than 0.7 dB. Most of the time is spent changing the transceiver configurations during the BER measurements. We administratively halted the transceiver for every configuration to ensure a stable transition, each requiring around a minute.

7. Future challenges

Although the wavelength dependence and fiber nonlinear effects were relatively small in our experimental system, it is highly expected that various line systems and fibers with various characteristics will be routed when providing DCX services. In such cases, techniques for estimating the wavelength dependence of amplifier gain and noise figure and nonlinear effects due to the fiber will be essential. Wavelength-dependent issues are expected to be solved by applying the latest technology, such as transfer learning, that predicts complex amplifier gain profiles [24].

We used TAI as the abstraction interface and CFP2-DCO as the coherent TRx, but the DCX needs to accommodate other form factors, such as QSFP-DD, which data center operators widely use. In the case of QSFP-DD, since the source code for QSFP-DD control has been opened in SONiC [25], it is desirable to utilize it instead of TAI. An architecture that efficiently accommodates different MSAs such as CFP MSA [18], Common Management Interface Specification (CMIS) [26], and Coherent-CMIS [27] will be required.

8. Conclusion

We proposed a technique to quickly and accurately estimate the GSNR of all possible EtE optical paths using a QoT probe channel that measures link by link at measurable, convenient, arbitrary modulation formats and modulators. We also proposed an approach to select the optimal mode in a short time based on the Gaussian noise approximation. Since this approach uses common parameters (BER, modulation format, and baud rate), they can be applied to all coherent TRx without being restricted to a specific device. These techniques enable DCX services that directly connect many-to-many user sites deployed in a two-dimensional plane via optical paths to respond to sudden traffic demands and to reconstruct optical path routes in

the event of disasters quickly. We identified issues related to user support/responsibility and interoperability/network robustness. Then, we proposed a Linux-based muxponder device software architecture with a DCX operator agent as a container to address the issues. We experimentally constructed three different paths by utilizing commercial optical transmission devices and field fibers; the accuracy estimated from the sum of the measurements for each link was 0.6 dB, and the wavelength-dependent error was about 0.3 dB. We combined WDM provisioning with the device software architecture in which users and carriers cooperate to optimize optical path transmission modes. Finally, we evaluated the time required for link quality estimation to enable EtE optical path margin designing and remote configuration of user muxponders. We provisioned two routes utilizing field fibers at 32 km and 122 km distances, assuming a 400G bandwidth request from a user. Our controller successfully selected the single λ_b 400G DP-16QAM path for the short route, and the two λ_b 200G DP-QPSK paths for the long route within 6 minutes automatically. The estimated and measured Q-factor (BER) differences were less than 0.7 dB.

Funding Information. NSF grants CNS-1827923, OAC-2029295, CNS-2112562, CNS-2128638, EEC-2133516, CNS-2211944, NSF Grant CNS-2148128 and by funds from federal agency and industry partners as specified in the Resilient & Intelligent NextG Systems (RINGS) program, and Science Foundation Ireland under Grant #13/RC/2077 P2.

Acknowledgment. We thank Rob Lane and the CRF team (Columbia), Lumentum, FOC, and the Telecom Infra Project OOPT-PSE working group.

References

1. IOWN Global Forum. (2023). Open APN architecture PoC reference, [Online]. Available: <https://iowngf.org/technology/> (visited on 08/05/2023).
2. Optical Internetworking Forum. (2023). 400ZR, Management/CMIS, [Online]. Available: <https://www.oiforum.com/> (visited on 09/06/2023).
3. OpenROADM MSA. (Aug. 2022). Open ROADM MSA specification ver 5.1, [Online]. Available: <https://openroadm.org/> (visited on 5/01/2023).
4. OpenZR+. (2023). [Online]. Available: <https://openzrplus.org/> (visited on 09/06/2023).
5. Telecom Infra Project. (2023). Phoenix: An open white-box L0/L1 transponder, [Online]. Available: <https://telecominfraproject.com/oopt/> (visited on 08/05/2023).
6. Telecom Infra Project. (2023). Goldstone: Goldstone open NOS, [Online]. Available: <https://github.com/oopt-goldstone/goldstone-mgmt> (visited on 05/01/2023).
7. Telecom Infra Project. (2023). TAI: Transponder abstraction interface, [Online]. Available: <https://github.com/Telecominfraproject/oopt-tai> (visited on 04/27/2023).
8. IOWN Global Forum. (2023). Open All-Photonic Network Functional Architecture, [Online]. Available: <https://iowngf.org/technology/> (visited on 08/05/2023).
9. Payman Samadi, Matteo Fiorani, Yiwen Shen, Lena Wosinska, and Keren Bergman, "Flexible architecture and autonomous control plane for metro-scale geographically distributed data centers," J. Lightwave Technology, vol. 35, no. 6, March 15, 2017.
10. Min Ju, Yuanhao Liu, Fen Zhou, and Shilin Xiao, "Disaster-resilient and distance-adaptive services provisioning in elastic optical inter-data

- center networks," J. Lightwave Technology, vol. 40, no. 13, July 1, 2022.
11. Kaida Kaeval, Tobias Fehenberger, Jim Zou, Sander Lars Jansen, Klaus Grobe, Helmut Griesser, Jorg-Peter Elbers, Marko Tikas, and Gert Jervan, "QoT assessment of the optical spectrum as a service in disaggregated network scenarios," J. Opt. Commun. Netw. Vol. 13, no. 10, Oct. 2021.
 12. Kaida Kaeval, Sander Lars Jansen, Florian Spinty, Klaus Grobe, Helmut Griesser, Tobias Fehenberger, Marko Tikas, and Gert Jervan, "Characterization of the optical spectrum as a service," J. Opt. Commun. Netw. Vol. 14, no. 5, pp. 398-410, 2022.
 13. Kaida Kaeval, Jani Myyry, Klaus Grobe, Helmut Griebler, and Gert Jervan, "Concatenated GSNR profiles for end-to-end performance estimations in disaggregated networks," in Optical Fiber Communication Conference (2022).
 14. H. Nishizawa, T. Sasai, T. Inoue, K. Anazawa, T. Mano, K. Kitamura, Y. Sone, T. Inui, and K. Takasugi, "Dynamic optical path provisioning for alien access links: Architecture, demonstration, and challenges," IEEE Communications Magazine, pp. 1–7, 2023. DOI: 10.1109/MCOM.006.2200567.
 15. Toru Mano, Andrea D'Amico, Emanuele Virgillito, Giacomo Borraccini, Yue-Kai Huang, Kazuya Anazawa, Hideki Nishizawa, Ting Wang, Koji Asahi, and Vittorio Curri, "Modeling transceiver ber-osnr characteristic for qot estimation in short-reach systems," in Proceedings of the International Conference on Optical Network Design and Modeling (ONDM), to appear, 2023.
 16. Vittorio Curri, "GNPy model of the physical layer for open and disaggregated optical networking [Invited]," JOCN, Vol. 14, Issue 6, pp. C92-C104 (2022).
 17. Openconfig. (2023). Terminal device properties found issues – New release proposed v0.2.0, [Online] Available: <https://github.com/openconfig/public/issues/910> (visited on 08/30/2023).
 18. CFP MSA Management Interface Specification Version 2.6, March 24, 2017, https://cfp-msa.org/wp-content/uploads/2022/10/CFP_MSA_MIS_V2p6r06a.pdf
 19. Chuan Qin, Binbin Guan, Kyle Edwards, Jian Kong, Ryan Morgan, Yawei Yin, Avinash Pathak, Mounika Banda, Sridharan J, Govardan Chandrababu, Jeetesh Jain, Jamie Gaudette, "Interoperable 400ZR Deployment at Cloud Scale," in Optical Fiber Communication Conference (OFC) 2023, Optica Publishing Group, 2023, W3H.2.
 20. Alessio Ferrari, Mark Filer, Karthikeyan Balasubramanian, Yawei Yin, Esther Le Rouzic, Jan Kundrát, Gert Grammel, Gabriele Galimberti, and Vittorio Curri, "GNPy: an open source application for physical layer aware open optical networks," vol. 12, issue 6, pp. C31-C40 2020.
 21. D. Raychaudhuri, I. Seskar, G. Zussman, T. Korakis, D. Kilper, T. Chen, J. Kolodziejewski, M. Sherman, Z. Kostic, X. Gu, H. Krishnaswamy, S. Maheshwari, P. Skrimponis, and C. Gutterman, "Challenge: COSMOS: A city-scale programmable testbed for experimentation with advanced wireless," in Proc. ACM MobiCom'20, 2020
 22. T. Chen, J. Yu, A. Minakhmetov, C. Gutterman, M. Sherman, S. Zhu, S. Santaniello, A. Biswas, I. Seskar, G. Zussman, and D. Kilper, "A software-defined programmable testbed for beyond 5g optical-wireless experimentation at city-scale", IEEE Network, vol. 36, no. 2, pp. 90–99, 2022. DOI: 10.1109 / MNET. 006. 2100605.
 23. Y. K. Huang, Z. Wang, E. Ip, Z. Qi, G. Zussman, D. Kilper, K. Asahi, H. Kageshima, Y. Aono, and T. Chen, "Field trial of coexistence and simultaneous switching of real-time fiber sensing and 400GbE supporting DCI and 5G mobile services," in Proc. IEEE/OPTICA Optical Fiber Communication Conference (OFC'23), W3H.4, Mar. 2023.
 24. Z. Wang, D. Kilper, and T. Chen, "Transfer learning based roadm edfa wavelength-dependent gain prediction using minimized data collection," in Optical Fiber Communication Conference (OFC) 2023, Optica Publishing Group, 2023, Th2A.1.
 25. Linux Foundation project. (2023). SONiC: Software for Open Networking in the Cloud, [Online]. Available: <https://sonicfoundation.dev/> (visited on 09/1/2023).
 26. Common Management Interface Specification (CMIS) Revision 5.2, April 27, 2022, <https://www.oiforum.com/wp-content/uploads/OIF-CMIS-05.2.pdf>
 27. Implementation Agreement for Coherent CMIS, OIF-C-CMIS-01.0, Jan. 14, 2020, <https://www.oiforum.com/wp-content/uploads/OIF-C-CMIS-01.0.pdf>